

Difference between Enzymatic and Chemical N-methylations of Protoberberine-Type Alkaloid, Dependent on the Stereoisomer of (−)-*N*-methyl-7,8,13,13a-tetrahydroberberinium Salt

Miyoko Kamigauchi,* Mayumi Yoshida, Yuko Noda, Jujiro Nishijo, Yasuko In,† Koji Tomoo,† Hirofumi Ohishi,† and Toshimasa Ishida†

Department of Physical Chemistry, Kobe Pharmaceutical University,
4-19-1 Motoyama-kitamachi, Higashinada-ku, Kobe 658-8558

†Osaka University of Pharmaceutical Sciences, 4-20-1 Nasahara, Takatsuki, Osaka 569-1094

(Received September 4, 2002)

A possible relation between the stereostructure of (−)-(13a*S*)-tetrahydroberberine (**1**) and its enzymatic/chemical N-methylation, an important biosynthetic reaction to isoquinoline alkaloids in plants, was examined by CD spectroscopic, X-ray crystallographic, and energy calculation methods. The CD measurements indicated that **1** has two conformers (*cis* and *trans*) concerning the ring junction of the quinolizidine skeleton, and exist with a *cis*/*trans* ratio of about 1/4 in a diethyl ether:2-methylbutane:ethanol (5:5:2) mixture. The dimensional/conformational difference between these *cis* and *trans* conformers was clarified by the X-ray crystal-structure analyses of two stereoisomers of N-methylated **1** (**3** and **4**). By using these structural parameters, the progress of N-methylation was simulated by energy profile calculations, suggesting that the *cis* and *trans* conformers are the major substrate for the enzymatic and chemical N-methylation reactions, respectively. Taking these results and the simulation of N-methylation of **1** by *S*-adenosyl-L-methionine at the binding pocket of N-methyltransferase into consideration, different pathways for chemical and enzymatic N-methylations of **1** have been proposed.

Isoquinoline alkaloids[1] in plants, such as morphine- and protoberberine-type alkaloids, are biosynthesized from an aromatic amino acid via L-dopa and dopamine.[2] Their existence in mammalian cells was recently reported, which stimulated a study of their biosyntheses and biological functions.[3,4] It is especially important to clarify the biosynthetic mechanism of protoberberine-type alkaloid to protopine-type via an *N*-methyl-protoberberinium-type intermediate, because of its major metabolic pathway.[5,6] Although tetrahydroberberine[7] takes two stereoisomers of (−)-(13a*S*) (**1**) and (+)-(13a*R*) (**2**), due to the asymmetric carbon, C(13a), the population of the former isomer is overwhelming in plants. As for the metabolic pathway of **1**, a stereo-specific route of **1** to (−)-*cis*-*N*-methyltetrahydroberberinium (**3**) (Fig. 1) was already established in the cell cultures, intact plants of *Macleaya cordata* (*papaveraceae*),[8] and other related plants.[6]

On the other hand, the stereochemistry on N-methylation of **1** remains to be clarified, i.e., the reason why only the *cis* form of **1** occurs selectively led to the biosynthesis of **3**, not **4**. Since **1** could take two different *cis* and *trans* B/C (*chair*/*chair*) conformers, its N-methylation is thought to produce two different molecules, **3** and **4**. In living cells, however, only **3** is stereospecifically biosynthesized; this is in contrast with the general chemical synthesis, in which the N-methylation of **1/2** by methyl iodide leads to **4/6** as the main product, respectively; the reaction to **3/5** is always minor.[8] This fact means that the N-methylation of tetrahydroberberine in plants is stereoselectively performed by the collaboration of *S*-adenosyl-L-methionine (SAM)[9–11] and (*S*)-7,8,13,13a-tetrahydroberberine-*N*-methyltransferase,[12,13] although this enzyme has not yet been isolated.

In an effort to find a clue why only **3**, not **4**, is selectively biosynthesized from **1** in living cells, the stereostructural and energetic features of **1**, **3**, and **4** were investigated by the CD spectral, X-ray crystal structural, and energy calculation methods. This paper deals with these results, together with the conformer-dependent reaction of **1** for its chemical and enzymatic N-methylations.

Results

CD Spectra of 1, 3, and 4. Since it has been reported by the CD[14] and NMR[15] measurements, and X-ray analysis[16] that **1** always takes a *trans* B(*chair*)/C(*chair*) conformation in solution as well as in the solid state, a protoberberine-type alkaloid bearing four oxygen atoms at positions 2, 3, 9, and 10 could be considered to preferentially adopt such a single *trans* conformer. However, the quinolizidine skeleton in the alkaloid appears to be relatively flexible due to a lone electron pair on the N(7) atom at the B/C ring joint moiety and, therefore, would be able to adopt both the *cis* and *trans* chair/chair conformations (Fig. 2). In fact, we already clarified[15] by IR and NMR methods that the derivatives of capaurine, 1-hydroxylprotoberberine type alkaloid, exist as an equilibrium state between the *cis* and *trans* conformers in solution. Thus, the possibility of **1** taking both conformers was reinvestigated by CD spectroscopic measurements.

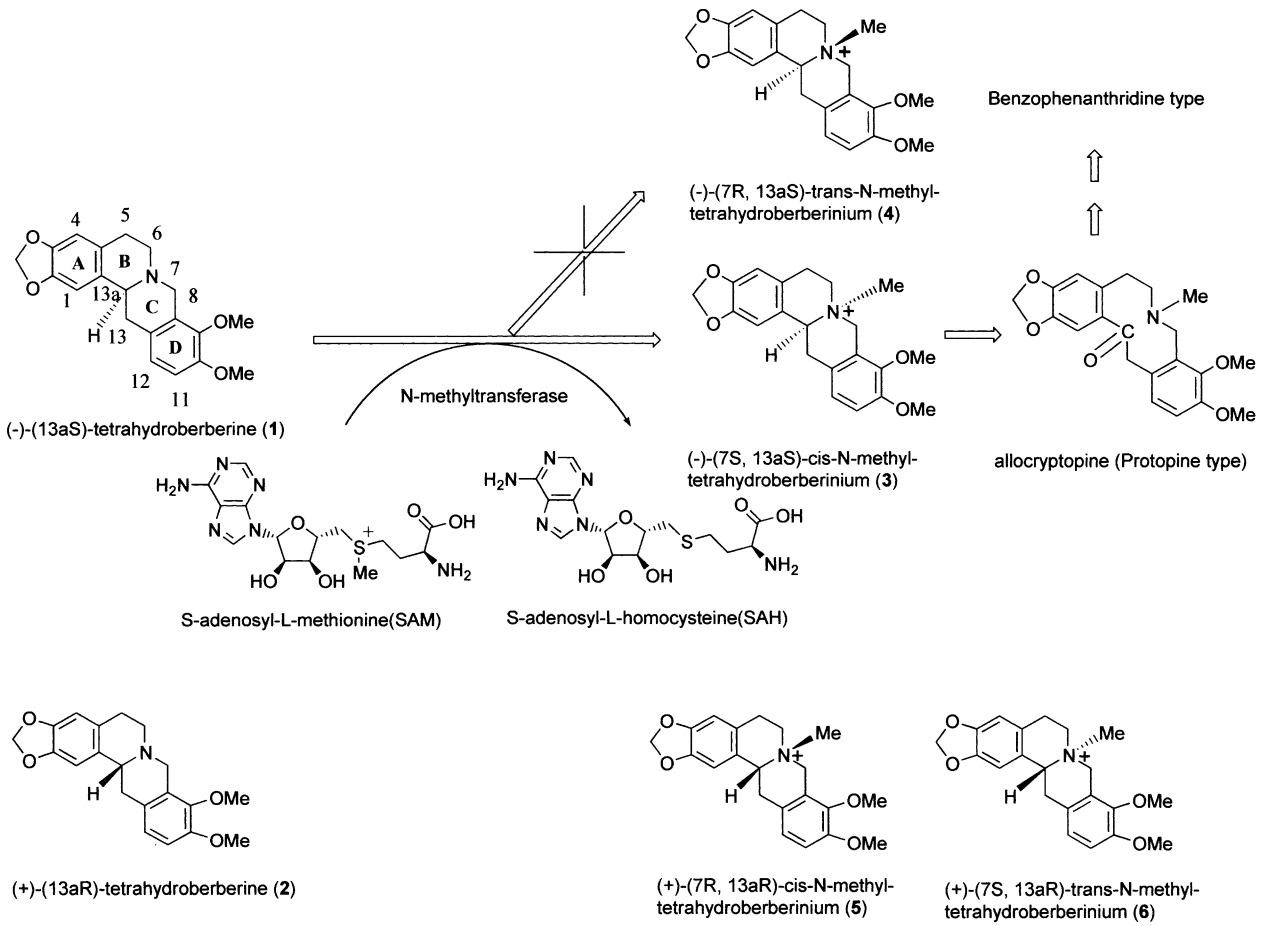

Fig. 1. Schematic metabolic pathway of **1** to **3** in *Macleaya cordata* and chemical structures of **1**–**6**. The atomic numbering of **1** used in this work is also given. Other related alkaloids are also shown for reference.

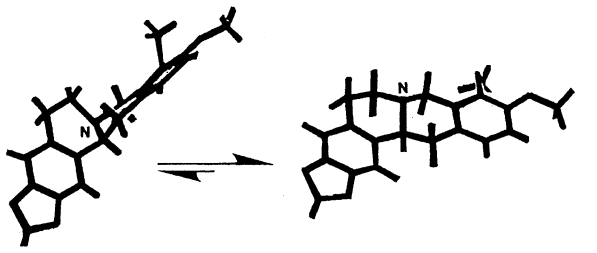

Fig. 2. Conformational equilibrium of *cis* and *trans* B(*chair*)/C(*chair*) of **1**.

Previously, we clarified[17] the relationship between the *cis*/*trans* conjunction at the B/C ring moiety and the CD spectrum for the hexahydrobenzo[c]phenanthridine-type alkaloid, which has a similar skeleton as the protoberberine type. That is to say, the CD spectrum enables a distinction between the *cis* and *trans* conformers, because the band is dependent on the dihedral angle between the A and D aromatic rings in the molecule. Therefore, the CD spectral features of the *cis* and *trans* conformers of **1** were estimated using *cis* **3** and *trans* **4**, based on the relationship between the *cis*/*trans* conformer and the CD band of hexahydrobenzo[c]phenanthridine. The CD spectra (Fig. 3a) showed three Cotton peaks [negative (205 nm), negative (235 nm), and negative (285 nm) peaks for *cis* **3** and negative (207 nm), negative (233 nm), and positive (286 nm) ones for *trans* **4**], corresponding to the β-, p-, and α-bands, respectively. The first two Cotton peaks could reflect the 13a-*S* absolute configuration, and the last one (α-band) the overall molecular conformation, respectively. The weak negative α-band ($\sim$300 nm) of **1** at 25 °C increases with decreasing the temperature (Fig. 3b). This clearly indicates that the population of the *cis* conformer increases as the temperature decreases. Based on related literature,[18–21] it could be estimated that ΔG^0 at 25 °C is about 3 kJ mol^{-1} from the CD intensity, and thus **1** is in equilibrium with the *cis* and *trans* conformers, where the ratio of the *cis*/*trans* conformer is about 1/4 at 25 °C.

In order to confirm the *cis*/*trans* population of **1** estimated from the CD intensity, the ratio of the chemical syntheses of the *cis* **3**/*trans* **4** from **1** by CH_3I was measured by the comparing *N*-methyl proton intensities of **3** and **4** with the ^{1}H NMR spectra. Consequently, the main product of *trans* **4** of over ca. 75% (Table 1) agrees well with the result of the CD spectra.

X-ray Crystal Structures of 3 and 4. In order to clarify the stereostructures of *cis* **3** and *trans* **4** in detail, these compounds, which were obtained by the N-methylation of **1** with CH_3I as stable molecules, were subjected to X-ray crystal-structure analyses. Their molecular conformations are shown in Fig. 4; both compounds showed almost the same bond

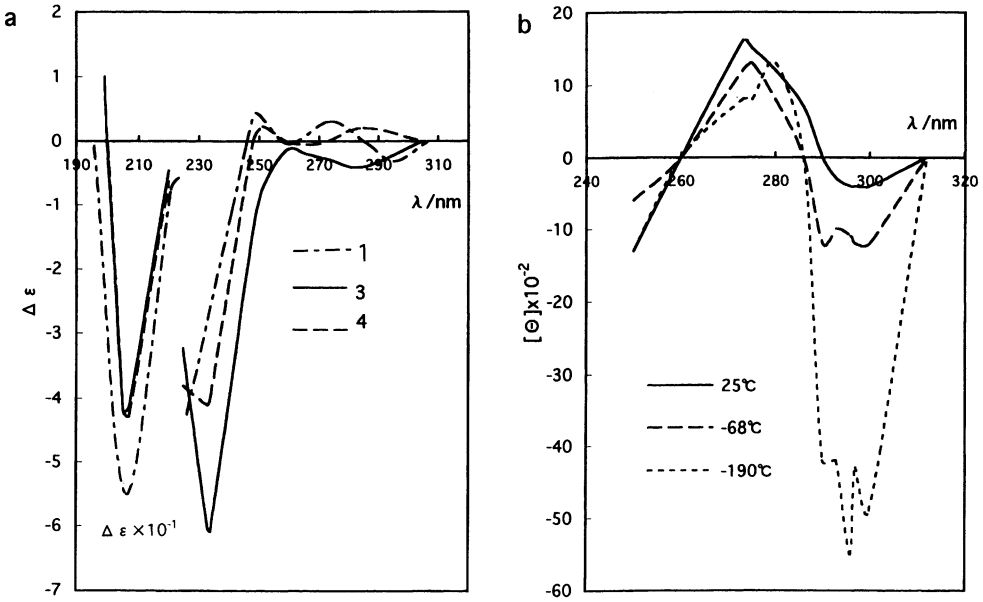

Fig. 3. (a) CD spectra of **1**, **3** and **4** in methanol at 25 °C. (b) Temperature-dependent CD spectra of **1** in diethyl ether:2-methylbutane:ethanol (5:5:2) mixture.

Table 1. Productive Population (%) of *cis* **3**/*trans* **4** in N-Methylation of **1** by CH_3I in Different Solvents

Entry	Solvent	Condition	**3**:**4** (%)[c]
1	acetone	sealed tube[a]	25:75
2	acetone	reflux[a]	28:72
3	chloroform	sealed tube[b]	12:88
4	chloroform	reflux[b]	16:84

a) The reaction was carried out at 55 °C. b) The reaction was carried out at 60 °C. c) Determined by ^{1}H NMR analysis.

lengths and angles. Although the B and C rings are both in a *half-chair* conformation, they differ in its ring conjunction: **3** takes a B/C *cis* form with a torsion angle of 176.6(8)° [C(13)–C(14)–N(7)–C(22)], whereas takes a **4** B/C *trans* form of 59(1)°; the dihedral angle between the A and D aromatic rings is 114(1)° for **3** and 173(1)° for **4**. Namely, **3** and **4** take the folded and planar conformations at the B/C ring junction, respectively, where the absolute configuration on the N(7) atom is 7-*S* for **3** and 7-*R* for **4**. A typical difference between their molecular conformations is that the *N*-methyl group of **4** is in a *quasi-axial* orientation toward the B and C rings, and thus possessing two 1,3-*diaxial*[22] correlated protons of C(5)–H and C(13)–H with respect to the *N*-methyl group, whereas that of **3** is in *quasi-axial* and *quasi-equatorial* directions toward rings B and C, respectively, and thus having a 1,3-*diaxial* correlated proton of C(5)–H. On the whole, the *N*-methyl group of **4** is directed to the β side crowded with hydrogen atoms, whereas that of **3** is located at the α side having a relatively large open space.

Energy Calculations. The *trans* B/C conformers of the N-unmethylated and -methylated protoberberine compounds would be more stable than the *cis* ones, as judged from the melting points of **3** and **4** and the production ratio of their syntheses. The CD spectra also showed that the *trans* conformer

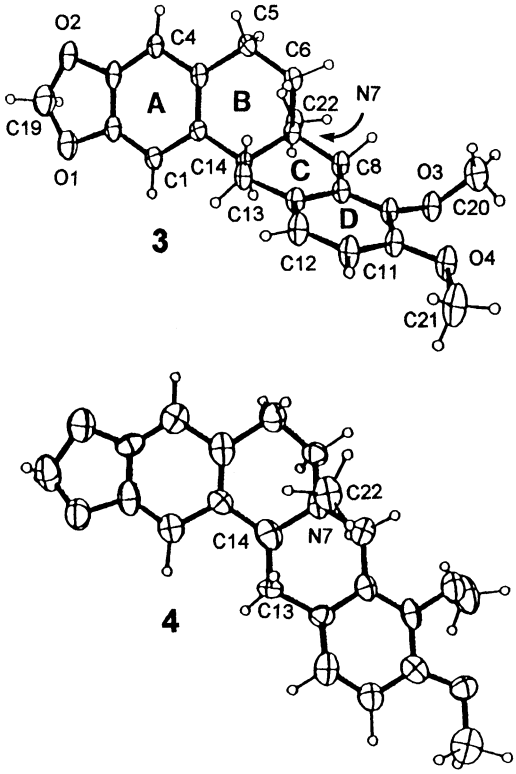

Fig. 4. Stereoscopic conformations of **3** and **4**. C(14) of the crystal analysis data shows the carbon equal to skeletal numbering C(13a). The ellipsoids are drawn at 50% probability. Open circles represent hydrogen atoms.

is predominant for **1**, and that *trans* **4** is the main product in the chemical N- methylation of **1**. In contrast, **1** is usually metabolized to *cis* **3** in plants and cell cultures (Fig. 1), in spite of the above-mentioned chemical and spectral disadvantages. In order to investigate whether there is any energetic advantage in

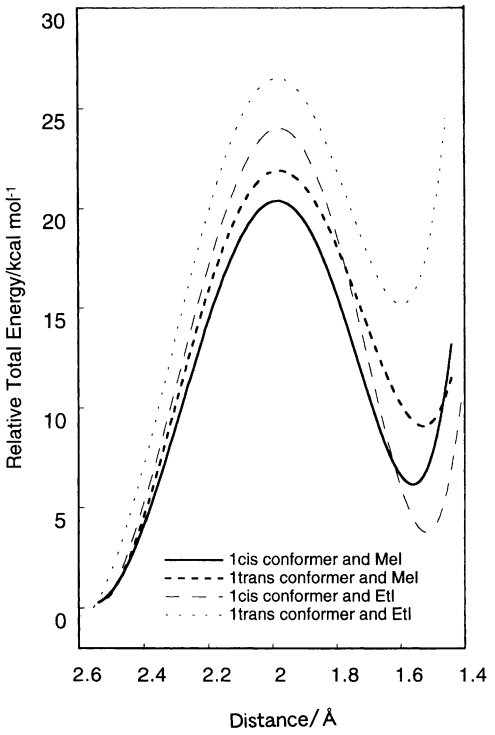

Fig. 5. Relative change of total energies (kcal mol^{-1}) of **1** and CH_3I or C_2H_5I as a function of N(**1**)–C (methyl/ethyl) distance. Each curve (r^2- value > 0.99) was prepared by the smoothing operation of 21 energy data calculated at 0.1 Å interval of the distance.

this biosynthetic pathway, we simulated the reaction pathway by the following three different energy calculations.

The first approach was to calculate the total energies of **1**, **3**, and **4** by molecular-orbital calculations (MOPAC/PM3 Var.6[23]). The result showed that *trans* **4** is more stable than *cis* **3**, which agrees with the synthetic result, i.e., *trans* **4** as the main product in the N-methylation of **1**. The second approach was to prepare an energy profile for the N-methylation of **1** by CH_3I as a function of the N–CH_3 distance. The calculations were performed on a MOPAC/INTER module[24] for two transition routes of the *cis* **1** → *cis* **3** and *trans* **1** → *trans* **4** conformers, where the distance between the N(7) and C(CH_3–I) atoms was changed from 2.5 Å to 1.4 Å at an interval of 0.1 Å. The results given in Fig. 5 show that (i) there was an energy difference of 7.53 kJ mol^{-1} at the transition state of N(**1**)–C(CH_3I) = 2 Å between both reaction routes and (ii) that the *cis* conformer route was more advantageous than the *trans* one. Similar results were also obtained for the N-alkylation of **1** by CH_3CH_2I (Fig. 5). To further confirm the preferred transition of the *cis* **1** → *cis* **3** route over the *trans* **1** → *trans* **4** route, the N-methylations of the *cis* and *trans* **1** conformers by SAM were simulated using the same approach; the results are given in Fig. 6. The transition energy (distance = 1.7 Å) of the *cis* route was lower by 204.54 kJ mol^{-1} than that of the *trans* one, suggesting that the transition via a *cis* conformer is profitable for N-alkylation by SAM, similar to the cases of CH_3I and C_2H_5I. The same conclusion was also obtained by the third approach, i.e., the calculation of the frontier electron density. In order to evaluate the reactivity of the N atom of the *cis* or *trans* **1** conformer toward the electrophilic reaction, the frontier electron density was calculated. Consequently, the coefficient 1.2710 eV of the *cis* conformer was larger than the 1.0726 eV of the *trans* conformer, indicating that the N-methylation reactivity on the *cis* **1** conformer is more active than that on the *trans* **1** conformer.

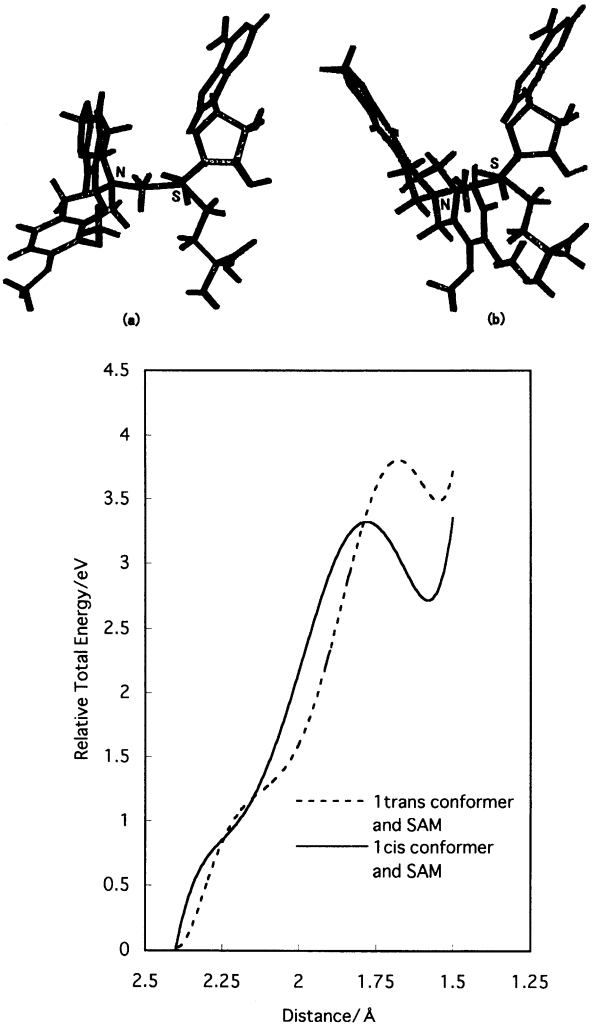

Fig. 6. Relative change of total energies (eV) of **1** and SAM as a function of N (7)–CH_3–S (SAM) distance. Each curve (r^2- value > 0.98) was prepared by the smoothing operation of 21 energy data calculated at 0.1 Å interval of the distance. Molecular conformations of *cis* **1** conformer–SAM (a) and *trans* **1** conformer–SAM (b) intermediates (N–C distance = 1.7 Å) are also shown.

Discussion

The chemical N-methylation of **1** by CH_3I resulted in the formation of *trans* **4** as a main product, namely ca. 75% of *trans* **4** and 25% of *cis* **3**. In contrast, it has been reported that the enzymatic N-methylation of **1** is stereoselectively transformed into *cis* **3** (Fig. 1). In order to elucidate this difference, the stereostructures of **1**, **3**, and **4** were analyzed by CD spectral and X-ray crystal analyses, and their energetic properties were investigated by molecular energy calculations.

Although *N*-methyl-tetrahydroberberinium is positioned at a

central part of the biosynthesis of the protoberberine-type alkaloid, its stereospecificity in the biosynthetic pathway is far from being fully understood. The present results clarify (i) the coexistence of minor *cis* and major *trans* conformers of **1** in solution, (ii) their stereostructural features by the crystal structures of **3** and **4**, and (iii) the preference of the *trans* **1** → *trans* **4** route for chemical N-methylation, supported by a total-energy calculation and a chemical synthesis, and of the *cis* **1** → *cis* **3** route for enzymatic N-methylation by calculations of the transition energy and the frontier electron density. Taking these results into consideration, a possible scheme for the chemical and enzymatic N-methylations of **1** is given in Fig. 7. The nitrogen atom of the *cis* **1** conformer allows the lone electron pair in a *quasi-axial* direction with respect to ring B (*S* configuration), whereas that of the *trans* **1** conformer is in a reverse orientation. It could be said from the present results that the preference of the *trans* **1** conformer for chemical N-methylation is dependent on the population ratio between the *cis* and *trans* conformers of **1**, rather than the attacking of the CH_3I to the lone pair. In enzymatic N-methylation, on the other hand, the stereostructure of **1** becomes important in the reaction pathway, and the *cis* form, which has a lower energy for the transition state than the *trans* one, is preferentially selected for the reaction, in spite of its smaller population rate and energy stability. In actual enzymatic N-methylation, the reaction would be taken place at the substrate-binding pocket of (*S*)-7,8,13,13a-tetrahydroberberine-*N*-methyltransferase, where only the *cis* conformer of **1** is stereo-selectively accepted and methylated by the coenzyme SAM. A preliminary docking model of the *cis* **1** conformer into the pocket is shown in Fig. 8, which was built by using the atomic coordinate of glycine *N*-methyltransferase cocrystallized with SAM; the details will be reported elsewhere. It is important to note that the *cis* conformer of **1** is much more compactly packed into the pocket compared with the *trans* conformer.

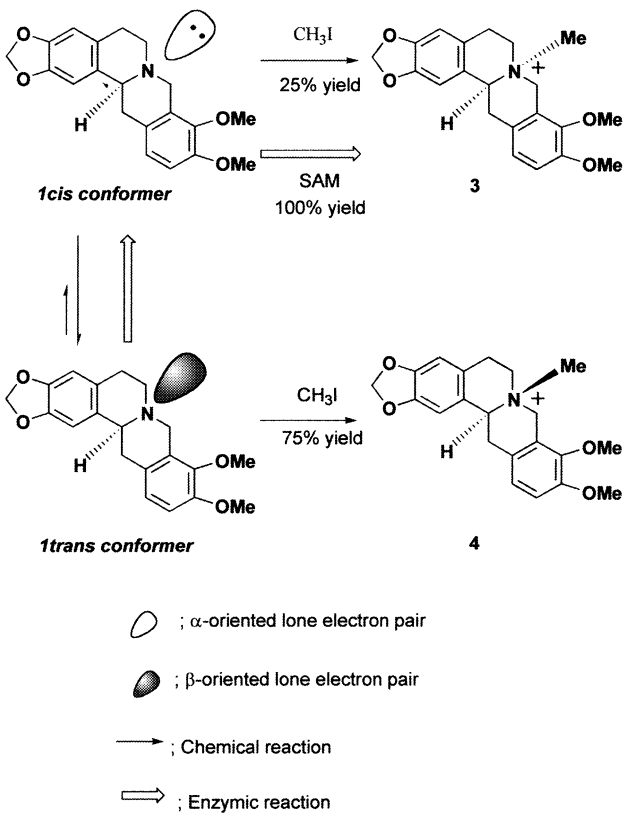

Fig. 7. Possible reaction route for N-methylation of *cis* and *trans* **1** conformers. Broad arrows: enzymatic reaction; narrow arrow: chemical reaction.

Many protoberberine-type alkaloids are included in plants, and play important functions in cells. The present work clari-

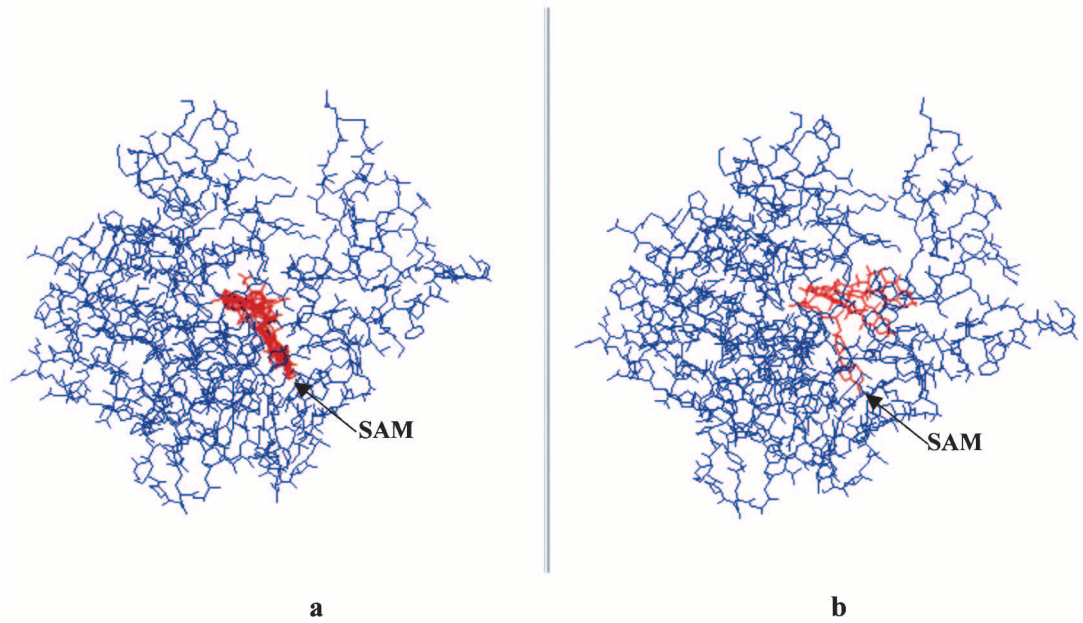

Fig. 8. Possible binding models of *cis* (a) or *trans* (b) **1** conformer–SAM intermediate at the binding pocket of *N*-methyltransferase (PDB code: 1XVA). The molecule of **1**–SAM intermediate is depicted by red color.

fied the difference between the chemical and enzymatic N-methylation processes of **1**, a representative protopine-type alkaloid. Since N-methylation occupies an important step in biosynthesizing such isoquinoline alkaloids, the results provide useful information for establishing their biosynthetic pathway, especially for considering the difference in chemical and enzymatic N-methylation.

Experimental

Material. (−)-7,8,13,13a-Tetrahydroberberine (**1**) and (+)-7,8,13,13a-tetrahydroberberine (**2**) were prepared from berberine chloride (Nacalai, Japan) by reduction with $NaBH_4$ and by optical resolution with (+)-10-camphorsulfonic acid. Also, (−)-(*cis*)-*N*-methyltetrahydro- berberinium iodide (**3**) and (−)-(*trans*)-*N*-methyltetrahydroberberinium iodide (**4**) were prepared from (−)-**1** according to the (racemic)-**1** synthesis.[8] **3**: mp 163.7–179.2 °C (MeOH), $[\alpha]_D$ −53.7° (*c* 1.1, MeOH); **4**: mp 251.8–255.8 °C (MeOH), $[\alpha]_D$ −83.6° (*c* 1.0, MeOH).

CD Spectral Data. The CD spectra were measured using a JASCO ORD/CD-5 or a JASCO-J 720 spectropolarimeter. A correction for the thermal contraction was not made. The CD Intensity $\Delta\varepsilon$ (nm) of **1** (0.265 mg/mL) in methanol; 25 °C; 0 (310), −0.29 (294), 0 (286), +0.36 (275), 0 (260), +0.51 (247.5), 0 (245), −4.33 (225), −55.45 (204.5), 0 (195); after acidified with HCl, 0 (310), −0.45 (295), −0.75 (282), −0.37 (260), 0 (250.5), −4.12 (225), −36.97 (206.5), 0 (195). CD Intensity of **1** (0.252 mg/mL) with different temperature in diethyl ether : 2-methylbutane : ethanol (5 : 5 : 2) mixture; 25 °C; −0.33 (300.5), −0.32 (293.5), +0.5 (275): −68 °C; −0.54 (300), −0.46 (290), +0.24 (275): −190 °C; −1.02 (301), −1.00 (294.5), −0.67 (289), +0.39 (273.5). CD Intensity of **3** (0.400 mg/mL) in methanol; 0 (302), −0.40 (285), −0.14 (261), −6.00 (235), −3.20 (226), −41.6 (205), 0 (197). CD Intensity of **4** (0.414 mg/mL) in methanol; 0 (300), +0.17 (286), 0 (273), −0.06 (267), 0 (258), +0.22 (251), 0 (248), −4.06 (233), −42.73 (207), 0 (199), +10.91 (195).

N-Methylation of 1 by CH_3I. In a 20mL-test tube with a coiled condenser or a pressurization test tube were dissolved **1** (10 mg) and CH_3I (500 μL) with stirring in acetone or $CHCl_3$ (5 mL); the tubes were maintained at a metal bath temperature of 58 or 65 °C for 6 h; each sample was evaporated to dryness under reduced pressure. After the addition CH_3OH-d_4 (1 mL, CEA 99.8%) into the reaction tube, a NMR measurement was made. The ^{1}H NMR spectra were measured in a CH_3OH-d_4 solution with tetramethylsilane (TMS) as the internal standard on a Varian VXR-500 (497.2 MHz) spectrometer. **3**; ^{1}H NMR (CH_3OH-d_4) δ 3.411 (3H, s, N-CH_3). **4**; ^{1}H NMR (CH_3OH-d_4) δ 3.062 (3H, s, N-CH_3).

X-ray Crystal Analyses of 3 and 4. Single crystals of (−)-**3**, and (−)-**4** were crystallized from methanol at room temperature as transparent plates and transparent prisms, respectively. Single crystals having dimensions of 0.6 × 0.6 × 0.9 mm^3 for **3**, and 0.7 × 0.3 × 0.8 mm^3 for **4** were used for X-ray studies. A summary of the crystallographic data is given in Table 2. The unit-cell dimensions were determined by a least-squares fit of the 2θ angles for 20 reflections of $10° < 2\theta < 65°$ for **3** and of $20° < 2\theta < 65°$ for **4**, which were measured by graphite-monochromated Mo Kα radiation (λ =0.7107 Å) for **3** and Cu Kα radiation (λ =1.5418 Å) for **4** on a Rigaku AFC-5R diffractometer. The intensity data ($2\theta \leqq 50°$ for **3** and $2\theta \leqq 130°$ for **4**) were collected using an ω-2θ scanning mode, where the background was counted for 5 s at both extremes of each reflection peak. The weak intensities [$F_0 < 2\sigma(F_0)$] were rescanned to ensure good counting statistics. Three standard reflections monitored for every 100 reflection intervals showed no significant deterioration ($< \pm 1.4\%$ for **3** and $< \pm 4.7\%$ for **4**). The observed intensities were corrected for Lorentz and polarization effects, but not for the absorption.

Table 2. Summary of Crystal Data and Intensity Collection Details of **3** and **4**

	3	**4**
Formula	$C_{21}H_{24}INO_4$ CH_3OH	$C_{21}H_{24}INO_4$ $2CH_3OH$
Formula weight	513.356	545.351
Crystal system	monoclinic	orthorhombic
Space group	$P2_1$	$P2_12_12_1$
a/Å	7.120(6)	14.011(3)
b/Å	14.381(3)	14.319(3)
c/Å	11.226(4)	12.111(4)
β/°	101.22(5)	
Volume/Å^3	1127.5(11)	2429.8 (11)
Z	2	4
D_x/g cm^{-3}	1.512	1.491
F(000)	520	1104
Crystal size/mm^3	0.6 × 0.6 × 0.9	0.7 × 0.3 × 0.8
No. of unique data measd	2077	2176
No. of data with $F_o > 2\sigma(F_o)$	1998	1711
No. of variables	266	286
R_f	0.052	0.096
R_{fw}	0.127	0.203

The structures were solved by direct methods using the program SHELXS-97.[25] The positional parameters of non-H atoms were refined by a full-matrix least-squares method with anisotropic thermal parameters. The hydrogen atoms were placed at an ideally reasonable position and fixed in the refinement. None of the positional parameters for non-H atoms shifted by more than their estimated standard deviations, and the residual electron densities in the final difference Fourier map were in the range of −0.907–0.791 eV Å^{-3} for **3** and −0.709–0.766 eV Å^{-3} for **4**, respectively. Crystallographic data have been deposited at the CCDC, 12 Union Road, Cambridge CB2 1EZ, UK and copies can be obtained on request, free of charge, by quoting the publication citation and the deposition numbers 182244 and 182245. All of the numerical calculations were performed on a Compaq Alpha Server DS10 computer at the Computation Center, Osaka University of Pharmaceutical Sciences.

Molecular Orbital Calculations. The heats of formation and the total energies of **3** and **4**, the Frontier orbital reaction coefficients of the nitrogen atom of the **1** *cis* and *trans* conformers, and the transition energy as a function of the N–CH_3 distance for the *cis* **1** → *cis* **3** and *trans* **1** → *trans* **4** reaction routes were calculated on a 4D Indy using MOPAC Var.6[23] in the MOL/MOLIS[24] system. The atomic coordinates of (−)-**3** and (−)-**4** were from the present X-ray results. The coordinates of the (−)-**1** *cis* conformer and the (−)-**1** *trans* conformer were built up from **3** and **4**, respectively. The atomic coordinate of SAM was built up from the X-ray result of SAH,[26] and those of CH_3I and CH_3CH_2I were from the default values in MOL/MOLIS.

Grid Map Simulated Annealing Docking. The conformation of *N*-Methyltransferase was constructed by using the crystal

structure of rat liver glycine *N*-methyltransferase complexed with SAM (PDB entry code 1XVA). The **1** *cis* or *trans* conformer was automatically placed at a position suitable for the reaction with SAM by the program MOE using a grid map simulated annealing docking method.[27] The complex was then energy-minimized by the program MOE using a molecular-mechanics force-field method. In detail, the grid map simulated in the annealing docking method was carried out between *N*-methyltransferase and the **1** *cis* or *trans* conformer, respectively. Force fields (MMFF94) were applied to both *N*-methyltransferase and the **1** *cis* or *trans* conformer, as previously described.[28] A simulating box (70 × 70 × 70 Å) was fixed around *N*-methyltransferase and the **1** *cis* or *trans* conformer, which were placed 8 Å apart. To increase the calculation accuracy, hydrogen atoms were added to both *N*-methyltransferase and the **1** *cis* or *trans* conformer. The grid map docking method was thereafter performed, giving 25 stable conformations between *N*-methyltransferase and the **1** *cis* or *trans* conformer, respectively.

The authors are grateful to Dr. K. Kuriyama and Mr. T. Iwata (Shionogi Research Laboratory, Co. Ltd.) for the CD spectral analyses.

References

1 T. Kametani, in "The Chemistry of the Isoquinoline Alkaloids," Vol.1, Hirokawa Publishing Company, Inc., Tokyo (1968): Vol.2, Sendai Inst. of Heterocyclic Chemistry, Sendai (1974).

2 C. W. W. Beecher and W. J. Kelleher, in "The Alkaloids; Chemical and Biological Perspectives," ed by S. W. Pelletier, Wiley, New York (1988), Vol. 6, p. 297.

3 M. A. Collins, "The Alkaloids: Mammalian Alkaloids," Academic Press, Inc. New York (1983), Vol. 21, pp. 329–358.

4 A. Brossi, "The Alkaloids: Mammalian Alkaloids II," Academic Press, Inc., New York (1993), Vol. 43, pp. 119–183.

5 a) N. Takao, K. Iwasa, M. Kamigauchi, and M. Sugiura, *Chem. Pharm. Bull.*, **24**, 2859 (1976). b) K. Iwasa, M. Kamigauchi, and N. Takao, *J. Nat. Prod.*, **51**, 1232 (1988). c) K. Iwasa, M. Kamigauchi, N. Takao, and M. Cushman, *J. Nat. Prod.*, **56**, 2053 (1993). d) M. Kamigauchi, Y. Noda, K. Iwasa, Z. Nishijo, T. Ishida, Y. In, and W. Wiegrebe, *Helv. Chim. Acta*, **77**, 243 (1994). e) K. Iwasa, Y. Kondoh, M. Kamigauchi, *J. Nat. Prod.*, **58**, 379 (1995). f) K. Iwasa, M. Kamigauchi, *Phytochemistry*, **41**, 1511 (1996).

6 a) M. Kamigauchi and K. Iwasa, "Biotechnology in Agriculture and Forestry, Vol. 26, Medicinal and Aromatic Plants VI," ed by Y. P. S. Bajaj, Spriner-Verlag, Berlin, Heidelberg (1994), pp. 93–105. b) K. Iwasa, "The Alkaloids: Chemistry and Pharmacology," ed by G. A. Cordell, Academic Press, Inc., New York (1995), Vol. 46, pp. 316–346.

7 R. H. F. Manske and H. L. Holmes, "The Alkaloids," Academic Press, London (1954), Vol. 4, p. 91.

8 N. Takao, M. Kamigauchi, and M. Okada, *Helv. Chim. Acta*, **66**, 473 (1983).

9 J. W. Cornforth, S. A. Reichard, P. Talalay, H.L.Carrell, and Jenny P.Glusker, *J. Am. Chem. Soc.*, **99**, 7292 (1977).

10 R. T. Borchardt, *J. Med. Chem.*, **19**, 1104 (1976).

11 V. Zappia, *J. Biol. Chem.*, **244**, 4499 (1969).

12 M. Rueffer and M. H. Zenk, *Tetrahedron Lett.*, **46**, 5603 (1986).

13 M. Rueffer, G. Zumstein, and M. H. Zenk, *Phytochemistry*, **29**, 3727 (1990).

14 G. Snatzke, J. JR. Hrubek, L. Hruban, A. Horeau, and F. Santavy, *Tetrahedron Lett.*, **26**, 5013 (1970).

15 N. Takao, K. Iwasa, M. Kamigauchi, and M. Sugiura, *Chem. Pharm. Bull.*, **25**, 1426 (1977).

16 T. Sakai, Z. Taira, M. Kamigauchi, and N. Takao, *Acta Crystallogr. Sect. C*, **43**, 98 (1987).

17 N. Takao, M. Kamigauchi, K. Iwasa, N. Morita, and K. Kuriyama, *Arch. Pharm. (Weinheim)*, **317**, 223 (1984).

18 A. Moscowitz, K. Wellman, and C. Djerassi, *J. Am. Chem. Soc.*, **85**, 3515 (1963).

19 S. Hagishita and K. Kuriyama, *J. Chem. Soc., Perkin Trans. 2*, 59 (1978).

20 T. Sato, M. Tada, T. Takahashi, I. Horibe, H. Ishii, T. Iwata, K. Kuriyama, Y. Tamura, and K. Tori, *Chem. Lett.*, **1977**, 1191.

21 M. Tada, T. Sato, T. Takahashi, K. Tori, I. Horibe, and K. Kuriyama, *J. Chem. Soc., Perkin Trans. 1*, 2695 (1981).

22 E. L. Eliel, N. L. Allinger, S. J. Angyal, and G. A. Morrison, "Conformational Analysis," John Wiley & Sons Inc., New York (1965).

23 J. J. P. Stewart, *J. Comput. Chem.*, **10**, 209 (1989).

24 "MOL/MOLIS; Molecular Orbital Analysis System," Daikin Industries, Ltd.

25 G. M. Sheldrick SHELXS-97, XP Molecular Graphics V 5.10, 1997, Brucker AXS.

26 T. Ishida, A. Tanaka, M. Inoue, T. Fujiwara, and K. Tomita, *J. Am. Chem. Soc.*, **104**, 7239 (1982).

27 Program MOE Chemical Computing Group Inc. CANADA (2002)

28 A. T. Halgren, *J. Comput. Chem.*, **20**, 730 (1999).